



Gamma in motion: Pattern reversal elicits stronger gamma-band responses than motion

Nicole Naue^a, Daniel Strüber^a, Ingo Fründ^b, Jeanette Schadow^c, Daniel Lenz^c, Stefan Rach^a, Ursula Körner^d, Christoph S. Herrmann^{a,*}

^a Department of Experimental Psychology, Carl-von-Ossietzky Universität, Ammerländer Heerstr. 114–118, 26129 Oldenburg, Germany

^b Modelling of Cognitive Processes, Berlin Institute of Technology and Bernstein Center for Computational Neuroscience, Franklinstr. 28/29, 10587 Berlin, Germany

^c Clinic of Child and Adolescent Psychiatry and Psychotherapy, Otto-von-Guericke-University, Leipziger Str. 44, 39120 Magdeburg, Germany

^d Honda Research Institute Europe, Carl-Legien-Str. 30, 63073 Offenbach/Main, Germany

ARTICLE INFO

Article history:

Received 21 July 2010

Revised 16 November 2010

Accepted 17 November 2010

Available online 2 December 2010

Keywords:

EEG

Gamma-band oscillations

40 Hz

Motion

Contrast

Fixational eye movements

ABSTRACT

Previous studies showed higher gamma-band responses (GBRs, ≈ 40 Hz) of the electroencephalogram (EEG) for moving compared to stationary stimuli. However, it is unclear whether this modulation by motion reflects a special responsiveness of the GBR to the stimulus feature “motion,” or whether GBR enhancements of similar magnitude can be elicited also by a salient change within a static stimulus that does not include motion.

Therefore, we measured the EEG of healthy subjects watching stationary square wave gratings of high contrast that either started to move or reversed their black and white pattern shortly after their onset. The strong contrast change of the pattern reversal represented a salient but motionless change within the grating that was compared to the onset of the stationary grating and the motion onset. Induced and evoked GBRs were analyzed for all three display conditions. In order to assess the influence of fixational eye movements on the induced GBRs, we also examined the time courses of microsaccade rates during the three display conditions.

Amplitudes of both evoked and induced GBRs were stronger for pattern reversal than for motion onset. There was no significant amplitude difference between the onsets of the stationary and moving gratings. However, mean frequencies of the induced GBR were ~ 10 Hz higher in response to the onsets of moving compared to stationary gratings. Furthermore, the modulations of the induced GBR did not parallel the modulations of microsaccade rate, indicating that our induced GBRs reflect neuronal processes.

These results suggest that, within the gamma-band range, the encoding of moving gratings in early visual cortex is primarily based on an upward frequency shift, whereas contrast changes within static gratings are reflected by amplitude enhancement.

© 2010 Elsevier Inc. All rights reserved.

Introduction

Since high-frequency oscillations were measured for the first time in the hedgehog (Adrian, 1942), gamma-band activity (20–80 Hz) gained tremendous interest in research and a lot of work has been conducted to characterize the functions of gamma-band oscillations in neuronal processes. There is accumulating evidence that gamma-band oscillations play a key role in fundamental brain functions including visual feature binding (Singer and Gray, 1995; Eckhorn, 1999; Gray, 1999; Herrmann et al., 1999), visual awareness (Ohla et al., 2007), memory (Herrmann et al., 2004a; Gruber and Müller, 2005; Busch et al., 2008), attention (Gruber et al., 1999; Tallon-Baudry et al., 2005), and learning (Miltner et al., 1999).

Gamma phenomena can be grouped into at least three categories: (i) spontaneous gamma oscillations, (ii) induced gamma-band responses (GBRs), and (iii) evoked GBRs (Başar-Eroglu et al., 1996). Spontaneous oscillations occur without correlation to sensory stimulation. Induced GBR consists of oscillatory bursts whose latency jitters from trial to trial. Thus, the temporal relationship with the stimulus onset is loose. In contrast, evoked GBRs occur in an earlier time window than induced GBRs and are phase-locked to the stimulus, i.e., show inter-trial phase synchrony. Simple sensory stimuli evoke GBRs in the cortex and subcortical structures (Başar et al., 1980; Demiralp et al., 1996). The strength of the evoked GBR is influenced by several physical features of visual stimuli such as size and eccentricity (Busch et al., 2004), visual contrast (Schadow et al., 2007), or spatial frequency (Fründ et al., 2007a). Furthermore, the evoked GBR is modulated by basic cognitive processes such as memory matching (Herrmann et al., 2004b) and attention (Busch et al., 2006; Debener et al., 2003; Fell et al., 2003). Induced GBRs, on

* Corresponding author. Tel.: +49 441 7984936; fax: +49 441 7983865.
E-mail address: christoph.herrmann@uni-oldenburg.de (C.S. Herrmann).

the other hand, have been associated with a wide range of cognitive processes including learning (Axmacher et al., 2006; Gruber and Müller, 2006; Gruber et al., 2001), perceptual binding (Engel et al., 1997), representation of objects (Lachaux et al., 2005; Tallon-Baudry, 1999), memory encoding and retrieval (Gruber et al., 2004; Sederberg et al., 2003), and working memory (Axmacher et al., 2007). It has been suggested that synchronous oscillations in the gamma-band could group action potentials from different neurons. Such grouping could be used to solve the binding problem (Singer and Gray, 1995), facilitate attentional processing (Fries et al., 2001), or enable hippocampal learning (Axmacher et al., 2006). Thus, while early evoked GBRs might reflect the encoding of physical attributes of the stimulus perceived, induced GBRs could play a crucial role in binding together brain areas performing the task (Tallon-Baudry, 1999). However, evoked and induced GBRs are electrophysiological correlates of cognitive processes that widely overlap (e.g., Engel et al., 2001; Fries et al., 2001; Herrmann et al., 2004a,b, see Herrmann et al., 2010 for a recent review).

With regard to motion, several animal studies (e.g., Gray et al., 1990; Kruse and Eckhorn, 1996; Schanze and Eckhorn, 1997) as well as human studies (e.g., Lutzenberger et al., 1995; Müller et al., 1997; Krishnan et al., 2005; Siegel et al., 2007) consistently reported enhanced induced GBRs for coherently moving stimuli compared to static ones or incoherent motion. For instance, Schanze and Eckhorn (1997) examined phase correlations using multiple microelectrode recordings in cat and monkey primary visual cortex. The authors presented moving light bars and reported significant phase correlations within the gamma–frequency range during stimulation. Another research group (Gray et al., 1990) also recorded intracranial responses of V1 in cats and found that moving stimuli were much more effective in eliciting oscillatory responses than stationary stimuli. However, in awake macaques, moving square-wave gratings generated GBRs of the same amplitude as stationary gratings, but at higher frequencies (Friedman-Hill et al., 2000). Recently, similar findings were reported in a human MEG study (Swettenham et al., 2009). In a human EEG study (Krishnan et al., 2005), random dot kinematograms were presented under three conditions: coherent motion, incoherent motion, and stationary stimulation. The authors reported that the magnitude of induced GBRs was greater in response to moving than static dot stimuli and more enhanced for coherent than incoherent motion. Increasing the level of motion coherence in a dynamic random dot pattern led to a monotonic increase of activity in the high gamma-band (60 to 100 Hz) in an MEG study (Siegel et al., 2007).

With one exception, all of the abovementioned studies restricted their analyses to induced GBR. Only one MEG study (Swettenham et al., 2009) analyzed both induced and evoked GBRs to moving stimuli. The authors presented stationary and drifting square-wave gratings in two separate sequence conditions. In the first condition, the drifting grating always followed the stationary grating within a trial, i.e., a previously stationary grating started to move. In the second condition, drifting and stationary gratings were presented in separate randomized trials, each preceded by a blank screen. Whereas no differential modulations were found for the evoked GBR, amplitudes of the induced GBR were significantly higher for moving gratings in the first sequence condition, but not in the second. Similarly for evoked GBRs, Zaehle et al. (2009) reported an increase of gamma-band amplitudes in response to moving gratings only for a simultaneous onset of grating and motion (i.e., the appearance of a moving grating following the presentation of a gray screen), whereas a pure motion onset of a previously stationary grating did not evoke a clear GBR. Together, the findings of Swettenham et al. (2009) and Zaehle et al. (2009) demonstrate that grating-based motion effects on the amplitude of gamma-band oscillations are modulated by the presentation mode and that evoked and induced GBRs might be inversely affected. Therefore, the question arises whether grating-based motion effects on the GBR are specific to the stimulus feature “motion” or whether they can be elicited also by other salient changes of the grating.

In order to answer this question in the present study, we introduced an additional condition beside stationary and moving patterns. We presented a simple square-wave grating of high contrast (grating onset condition), which either started to move (motion condition) or inverted its black and white stripes (pattern reversal condition) representing a strong contrast change. This presentation mode allowed a direct comparison between the pattern reversal and motion condition without confounding effects of stimulus onset. Furthermore, the presentation mode enhances the ecological validity of the paradigm in that it is more naturalistic to recognize a change in a stimulus that is already existent in the visual field than reacting on stimuli that suddenly appear in the central visual field. We analyzed the evoked and induced GBRs to the three conditions, onset of the grating, pattern reversal, and motion.

Recently, induced GBRs were suspected to be generated by microsaccades rather than reflecting neural responses (Yuval-Greenberg et al., 2008). Yuval-Greenberg et al. (2008) demonstrated that the typical transient amplitude increase of the EEG scalp-recorded induced GBR at about 200–300 ms after stimulus onset is related to the characteristic rebound of the microsaccade rate following a period of poststimulus microsaccadic inhibition (Engbert and Kliegl, 2003). In order to interpret induced GBRs in the present study, we conducted a second experiment with an eye-tracking system, assessing the time course of microsaccade rates in response to grating onset, pattern reversal, and motion.

Experiment 1

In the first experiment, we presented a stationary grating (grating onset), which after some time either started to drift downwards (motion) or which inverted its black and white stripes (pattern reversal). The pattern reversal condition served as an example of a salient change in the grating that does not include motion. Induced and evoked GBRs were analyzed for all three display conditions.

Materials and methods

Subjects

Fourteen university students (10 female), aged 18–32 years (mean=23.5; SD=3.67) participated in the study. All gave their written informed consent and were paid or received course credits for their participation. The subjects had normal or corrected-to-normal vision and reported no neurological or psychiatric disorders. The experiment was conducted in accordance with the Declaration of Helsinki concerning human experimentation.

Stimuli and procedure

Square-wave gratings with close to 100% Michelson contrast, a constant spatial frequency of 1.5 cpd and a diameter of 10° visual angle were generated using MATLAB R2006b. The gratings were overlaid with a gray mask simulating a circular aperture at the screen. A fixation cross, presented in the middle of the screen, served as a gaze fixation target during the whole trial. Fig. 1 schematically illustrates the sequence of events for a pattern reversal and motion trial, respectively. Each trial started with the onset of the grating (grating onset) that was presented for a pseudorandomly varying duration between 1500 and 1900 ms. After this variable time, two possible events could happen with equal probability. In one case, there was a single pattern reversal of the stripes (pattern reversal; see Fig. 1A), and in the other case, the stripes started to drift downwards (motion; see Fig. 1B) with a velocity of 1.75°/s. Single pictures were presented with a repetition rate of 33 Hz. The motion of the stripes persisted for 570 ms. Afterwards, the grating was stationary presented for additional 500 ms, then it disappeared and only the fixation cross remained during the 1000 ms inter-stimulus interval (ISI). In trials where the stripes reversed, the grating persisted on the screen for 1070 ms, keeping the trial length in both conditions

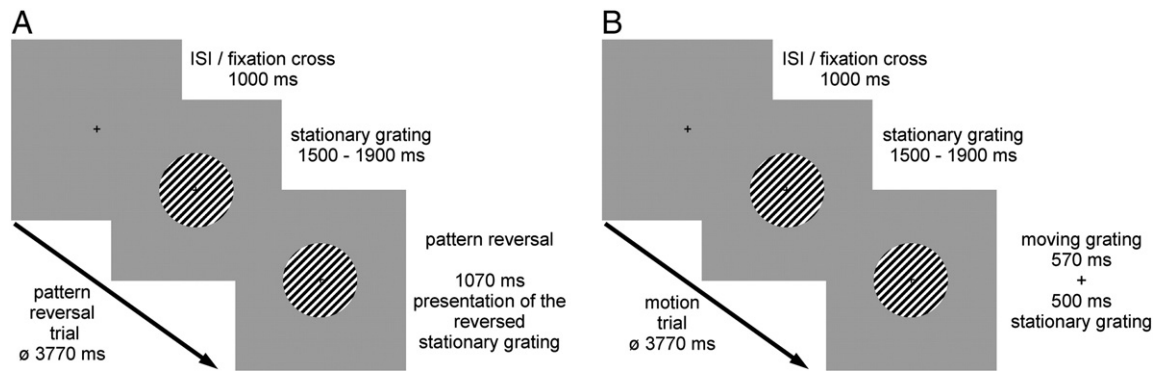


Fig. 1. Schematic illustration of a pattern reversal trial (A) and a motion trial (B). Each trial started with the onset of the grating, which was stationary presented for a pseudorandomly varying duration between 1500 and 1900 ms. Then the pattern reversal or motion of the stripes started. (A) In pattern reversal trials, the grating reversed its black and white stripes and then remained stationary for 1070 ms. (B) For motion trials, single pictures were presented for 570 ms with a repetition rate of 33 Hz and the last single picture persisted for 500 ms on the screen, resulting in an overall trial duration of 1070 ms, too. The subjects had to discriminate both events by corresponding button presses.

constant. The subjects had to discriminate pattern reversal from motion trials by corresponding button presses with the index fingers of both hands. A total of 200 trials were presented in pseudorandomized order, 100 trials for each condition.

Data acquisition

The experiment was conducted in an electrically shielded and sound attenuated room (IAC, Niederkrüchten, Germany). The stimulation monitor was placed outside the cabin behind an electrically shielded window. All devices inside the cabin were battery operated to avoid line frequency interference (50 Hz in Germany). EEG was recorded with a BrainAmp amplifier (Brain Products, Munich, Germany), using 64 sintered Ag/AgCl electrodes mounted in an elastic cap (EasyCap, Falk Minow Services, Munich, Germany) and placed according to the 10–10 system, with a reference placed at the right earlobe and ground electrode between Fz and Cz. Eye movement activity was measured from one electrode placed sub-orbitally to the left eye and another electrode lateral to the right eye. Electrode impedances were kept below 5 k Ω . Data were acquired with a band-pass filter of 0.016–250 Hz and a sampling rate of 500 Hz. Analog-digital conversion was performed at an amplitude resolution of 16 bit. Stimulus markers and EEG signals were stored on hard disk for further analysis. Digitized EEG data were transferred to a computer outside the recording cabin with a fiber optic cable. All data were re-referenced offline using an average reference of all electrodes except the channels T7 and T8, since they are susceptible for muscle artifacts, and the two electrodes measuring eye movements. An additional digital high-pass filter with a cutoff frequency of 0.5 Hz was applied offline to reduce slow shifts in the baseline. Averaging epochs lasted from 200 ms before to 1500 ms after grating onset and to 800 ms after pattern reversal or motion onset, respectively. Baseline activity was calculated in the interval from –200 to –100 ms and subtracted before averaging. An automatic artifact rejection was computed, excluding trials from averaging if the standard deviation within a moving 200ms time window exceeded 30 μ V in any channel. Subsequently, all epochs were also visually inspected for artifacts and rejected in case of eye movements, electrode drifts, or electromyographic activity.

Data analysis

For the analysis of reaction times, only trials with responses given between 200 and 1500 ms were included in the analysis. Trials with incorrect responses were excluded from the behavioral data analysis, as well as trials in which the reaction time (RT) exceeded two standard deviations from the mean. For comparison of the conditions, paired two-tailed *t*-tests were calculated.

For the analysis of gamma-band activity, a wavelet transform was computed by convolving the raw EEG signal with a complex-

modulated Gaussian (Herrmann et al., 1999). At 40 Hz, the wavelet had a time resolution of $2\sigma_t \approx 50$ ms and a frequency resolution of $2\sigma_f \approx 13$ Hz. The exact time–frequency resolution of the wavelet depended on the analyzed frequency. To analyze the evoked GBR, phase-locked to the stimulus, the wavelet transform was applied to the averaged event-related potential. For the non-phase-locked portion of the GBR, the wavelet transformation was first applied to each single trial and then the resulting absolute values of the wavelet transforms were averaged. This measure represents the total activity comprising the phase-locked (evoked) and non-phase-locked (induced) fractions of the GBR. The induced fraction can be identified by its absence in the evoked measure. The wavelet analysis was performed for each frequency bin in the gamma-frequency range (20–80 Hz). The resulting time–frequency representations were pooled into a region of interest (ROI) and averaged across electrodes, which exhibited the strongest GBRs after visual stimulation: PO3, POz, PO4, O1, Oz, and O2. For the evoked GBR, the individual gamma frequency for each subject was defined as the frequency showing the highest amplitude in the frequency range of 20 to 80 Hz and in the time interval between 40 and 180 ms after the onset of the grating, pattern reversal, and motion onset, respectively. The peak frequencies of the individually identified evoked GBRs ranged from 20 to 78 Hz (mean: 45.76 Hz, SD = 19.18 Hz). The peak amplitude for this individual frequency was used for further statistical analyses of the evoked GBR. The time–frequency window for peak detection of the induced GBR had to be restricted to the frequency range above 40 Hz, since otherwise the 33-Hz steady-state response in the motion condition would lie inside this late time window (see Fig. 3 right). For the induced GBR, the peak frequencies were determined for the same ROI in the frequency range from 40 to 80 Hz and in the time interval between 100 and 500 ms. The peak frequencies of the individually identified induced GBRs ranged from 41 to 79 Hz (mean: 58.52 Hz, SD = 8.08 Hz). The peak amplitude for this individual frequency was used for further statistical analyses of the induced GBR. We also tested whether the mean frequencies differed between display conditions. The statistical analysis of gamma-band activity was performed on the ROI. Effects of the different display conditions on the GBR were analyzed by means of a repeated measures ANOVA (factor condition: grating onset, pattern reversal, motion) applying the Greenhouse–Geisser correction method when appropriate. If the ANOVA yielded a significant effect, post hoc *t*-tests of specific comparisons were calculated. These post hoc tests were corrected for multiple comparisons according to Bonferroni's method.

Results and discussion

Behavioral results

The subjects responded with high accuracy in both conditions (pattern reversal: $94.57 \pm 3.25\%$ correct responses; motion: $95.86 \pm 0.90\%$

correct responses) with no significant difference between both conditions [$t(13) = -1.53, p = 0.150$]. Furthermore, the mean reaction times in both conditions (pattern reversal: 525.02 ± 65.89 ms; motion: 523.01 ± 72.57 ms) did not differ significantly [$t(13) = 0.17, p = 0.867$].

Gamma-band response

Each condition elicited a clearly visible evoked and induced GBR (see Figs. 2 and 3A, B). Furthermore, a steady-state response was visible in the motion condition, which lasted for the whole movement duration of the stripes (570 ms) and was due to the presentation of the single pictures representing the movement (see dashed box in Fig. 2B, bottom). The steady-state response was not subjected to formal analysis. The mean peak amplitudes and latencies of the evoked and induced GBR are listed in Table 1 for all display conditions.

Fig. 2 displays the evoked GBR, which differed significantly between display conditions with respect to both amplitude [$F(2,26) = 36.713, p < 0.001$] and peak latency [$F(2,26) = 28.810, p < 0.001$]. Post hoc paired two-tailed *t*-tests showed a significant amplitude difference between pattern reversal and motion [$t(13) = 6.98, p < 0.001$], as well as between pattern reversal and grating onset [$t(13) = 6.25, p < 0.001$], both with higher amplitudes in the pattern reversal condition. There was no significant difference between grating onset and motion [$t(13) = 1.00,$

$p = 1.0$]. The peak latencies differed significantly between pattern reversal and motion [$t(13) = -6.58, p < 0.001$], as well as between grating onset and motion [$t(13) = -5.24, p < 0.001$], both with a longer latency in the motion condition. There was no significant latency difference between grating onset and pattern reversal [$t(13) = 1.73, p = 0.321$].

Fig. 3A and B displays the induced GBR, which differed significantly between display conditions with respect to both amplitude [$F(2,26) = 3.854, p < 0.05$] and peak latency [$F(2,26) = 4.487, p < 0.05$]. Post hoc paired two-tailed *t*-tests showed a significant amplitude difference for pattern reversal and motion [$t(13) = 2.95, p < 0.05$], with higher amplitudes in the pattern reversal condition. There was no significant difference between grating onset and pattern reversal [$t(13) = 0.15, p = 1.0$] nor between grating onset and motion [$t(13) = 2.03, p = 0.192$]. The peak latencies of the induced GBR differed significantly between grating onset and motion [$t(13) = -2.97, p < 0.05$], with a shorter latency for grating onset. There was no latency difference between pattern reversal and motion [$t(13) = -0.48, p = 1.0$] and between grating onset and pattern reversal [$t(13) = -2.04, p = 0.189$].

In addition, we found indications of a sustained GBR for static and moving gratings. As can be seen in Fig. 3A, the induced GBR in the

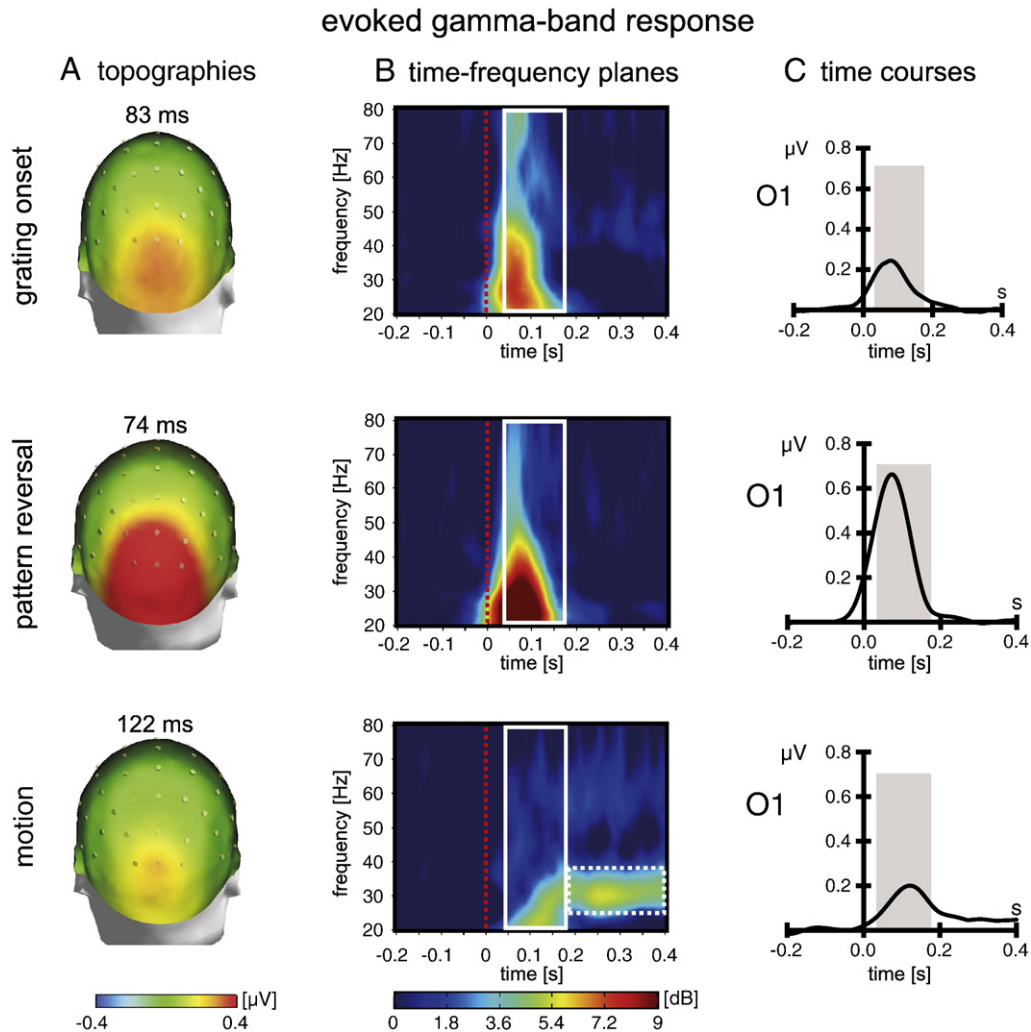


Fig. 2. Evoked gamma-band response (Experiment 1). Top row: onset of the grating; middle row: pattern reversal; bottom row: motion condition. (A) Topography of the evoked GBR at peak latencies. The scalp distribution of the evoked GBR shows its maximum at posterior electrodes. Amplitudes are clearly enhanced in the pattern reversal condition. (B) Time-frequency representations averaged across all subjects and the posterior ROI. The red dotted line represents the time point of grating onset, pattern reversal, and motion onset, respectively. The white boxes represent the window for statistical analysis of peak amplitudes. Note that the activity in the dashed box (bottom) represents a steady-state activity due to presentation of the single images that represent the motion. A stronger evoked GBR after pattern reversal is visible compared to grating and motion onset. (C) Time courses of the evoked GBR at electrode O1 averaged across all subjects. The gray bars represent the time window for statistical analysis.

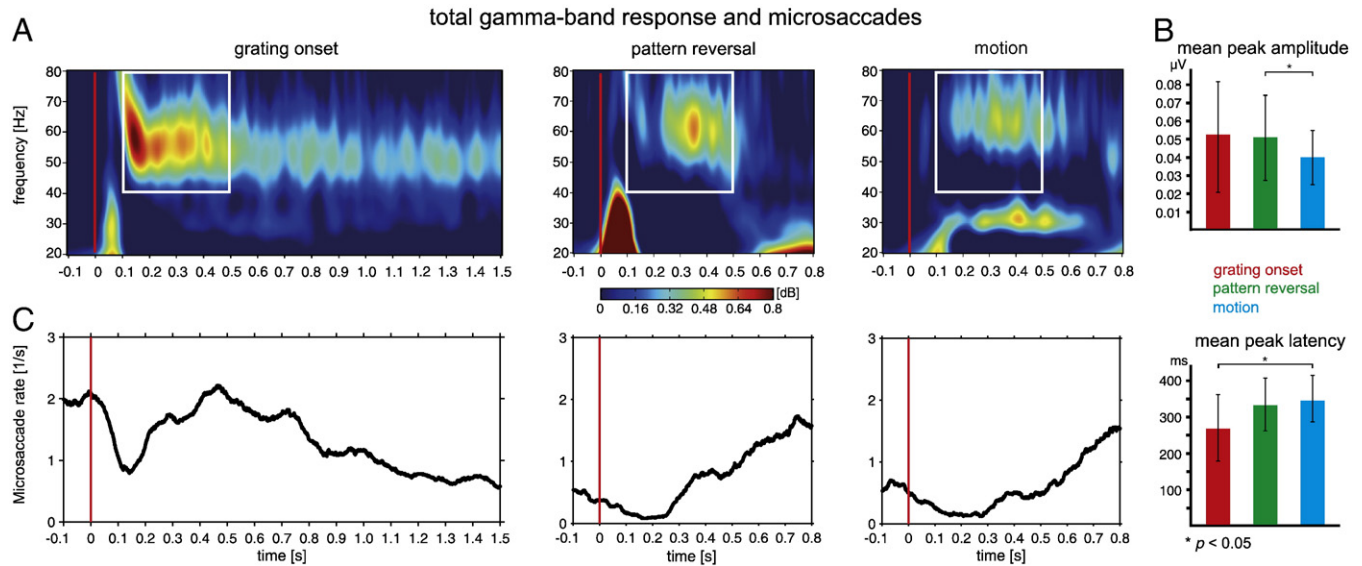


Fig. 3. Total gamma-band response (Experiment 1) and microsaccades (Experiment 2). (A) Time–frequency plots of the total GBR (comprising the evoked and induced GBR) averaged across all subjects and the posterior ROI. The white boxes represent the analysis window for the induced GBR. (B) Histogram of the mean peak amplitudes (top) and the mean peak latencies (bottom) of the induced GBR separately for each condition, averaged across all subjects and the ROI. Error bars denote the standard deviation. The asterisks indicate significant differences. Note that the seemingly stronger induced GBR in response to grating onset as visible in the time–frequency plots was due to only a few subjects and did not therefore influence the statistics. (C) Time course of microsaccades rate (per second) averaged across participants and smoothed with a moving time window of 100 ms. Note that neither the difference between conditions nor the latency of the maxima corresponds to the induced GBR.

grating onset condition occurs immediately after the evoked onset response at ~100 ms and then persists throughout the presented time range. Similarly for the motion condition, the induced GBR starts after the evoked motion onset response at ~150 ms and continues until ~550 ms following motion onset, which corresponds nicely to the 570 ms presentation time of the moving grating.

For the induced GBR, we also tested whether there are differences in the mean frequency of GBR between display conditions. The ANOVA yielded a significant effect of condition [$F(2,26) = 5.689$, $p < 0.05$]. Post hoc t -tests revealed a significant difference between grating and motion onset [$t(13) = -3.864$, $p < 0.01$], with higher frequencies in the motion condition, but not for the other comparisons [pattern reversal vs. motion: $t(13) = -1.01$, $p = 0.987$; pattern reversal vs. grating onset: $t(13) = 2.211$, $p = 0.138$].

The finding of higher amplitudes for both evoked and induced GBRs in response to pattern reversal compared to motion might indicate that a sudden contrast change within an object (pattern reversal) represents a more salient stimulus for the early visual system than motion. For the evoked GBR, this interpretation is in line with the shorter latency for pattern reversal, indicating a faster processing of pattern reversal compared to motion. For induced GBRs, peak latency was prolonged for motion and pattern reversal compared to grating onset, which might relate to differing task demands, since motion had to be discriminated from pattern reversal, whereas no task was required during the grating onset condition. Consistent with this interpretation, it has been shown that peak latency delays of the induced GBR are accompanied by recognition

delays due to increased discrimination difficulty (Martinovic et al., 2008).

Interestingly, our observation of higher gamma-band frequencies for moving as compared to static gratings in the absence of amplitude differences was also reported for V1 neuronal activity in the awake monkey (Friedman-Hill et al., 2000).

Experiment 2

In the second experiment, we measured eye movements in response to the same display conditions that have been used in Experiment 1. Because at the time of EEG measurements no eye tracker was available in our laboratory, we had to conduct this session separately with different participants. The purpose of this experiment was to examine whether microsaccade rates were differentially modulated by the display conditions. The results are used to estimate possible influences of microsaccades on the induced GBRs obtained in Experiment 1.

Methods

Subjects

Ten subjects (3 female), aged 23–44 years (mean = 31.8; SD = 7.38) with normal or corrected to-normal-vision and no reported neurological or psychiatric disorders participated in this experiment. The experiment was conducted in accordance with the

Table 1
Mean peak amplitudes and latencies of the evoked and induced GBR. The standard deviation (SD) is displayed in brackets.

Condition	Evoked GBR		Induced GBR	
	Mean Amplitude	Mean Peak latency	Mean Amplitude	Mean Peak latency
Grating onset	0.216 (± 0.123) μ V	83 (± 22) ms	0.052 (± 0.031) μ V	271 (± 92) ms
Pattern reversal	0.571 (± 0.281) μ V	74 (± 11) ms	0.051 (± 0.024) μ V	333 (± 71) ms
Motion	0.180 (± 0.114) μ V	122 (± 26) ms	0.040 (± 0.015) μ V	344 (± 65) ms

Declaration of Helsinki concerning human experimentation and participants gave their written informed consent.

Stimuli and procedure

Stimuli and procedure were the same as in Experiment 1.

Data acquisition

Participants were seated in a silent and dimly lit cabin with the head positioned on a chin rest at a distance of 60 cm from a computer screen. Binocular eye movements were recorded and saved for offline analysis using an EyeLink 2000 infrared videooculographic desk-mounted system (SR Research Ltd., Osgoode, ON, Canada). Eye position data for both eyes were sampled with a spatial resolution of 0.01° and a temporal resolution of 1000 Hz.

Data analysis

Data analysis for reaction time was the same as in Experiment 1.

Microsaccades were detected using an improved version (Engbert and Mergenthaler, 2006) of an algorithm proposed by Engbert and Kliegl (2003). The Matlab code is kindly provided at <http://www.agnld.uni-potsdam.de/~ralf/MS>. Microsaccade detection in a 2D velocity space utilized a threshold for peak velocity (VTHRES) of 5 SD and a minimum duration (MINDUR) of 3 data samples. Only binocular microsaccades (i.e., microsaccades detected in both eyes with temporal overlap) were considered for further analysis.

To compare the time course of microsaccade rates for different display conditions, we employed a non-parametric bootstrap procedure to estimate the variability of the microsaccade time courses. The bootstrap method is a Monte Carlo technique that generates simulated data sets by resampling from empirical data observed in the original experiment (Efron and Tibshirani, 1986). As we recorded eye movements from more than one subject, we had to apply the following nested resampling strategy to capture the variability across subjects and trials. We generated 2000 surrogate data sets as follows:

(1) draw a surrogate sample of 10 participants with replacement from the original set of participants; (2) for each of these 10 surrogate participants, draw 100 surrogate trials per condition with replacement; (3) for the resulting surrogate data, calculate the average for each condition across surrogate trials and participants and smooth with a time window of 100 ms. Repeating these 3 steps 2000 times resulted in a distribution of average time courses of microsaccade rates for each display condition. From these distributions, 68% confidence intervals (CI_{68}) were calculated by the bootstrap percentile method. CI_{68} confidence intervals span from the 16th to the 84th percentile of the bootstrap distribution, which approximately compares to ± 1 standard deviation of a Gaussian.

Results and discussion

Behavioral results

The subjects responded with high accuracy in both conditions (pattern reversal: $96.9 \pm 2.28\%$ correct responses; motion: $97.7 \pm 2.83\%$ correct responses). There was no difference between conditions [$t(9) = 0.91$, $p = 0.387$]. The mean reaction times in both conditions (pattern reversal: 680.99 ± 280.20 ms; motion: 714.42 ± 308.45 ms) did not differ significantly [$t(9) = 1.206$, $p = 0.258$].

Microsaccade rate

Fig. 4 shows the microsaccade rates per display condition for a single subject. Histograms represent saccade rate per second calculated in 25 ms bins. The red curve represents the microsaccades' rate (per second) smoothed with a moving time window of 100 ms.

The mean rate of microsaccades averaged across all subjects is given in Fig 3C for each display condition. As can be seen, there is a marked difference in the time course of microsaccades between grating onset and the two other conditions. The onset of the grating elicited an initial decrease of the microsaccade rate from about two per second to below one per second about 150 ms after grating onset.

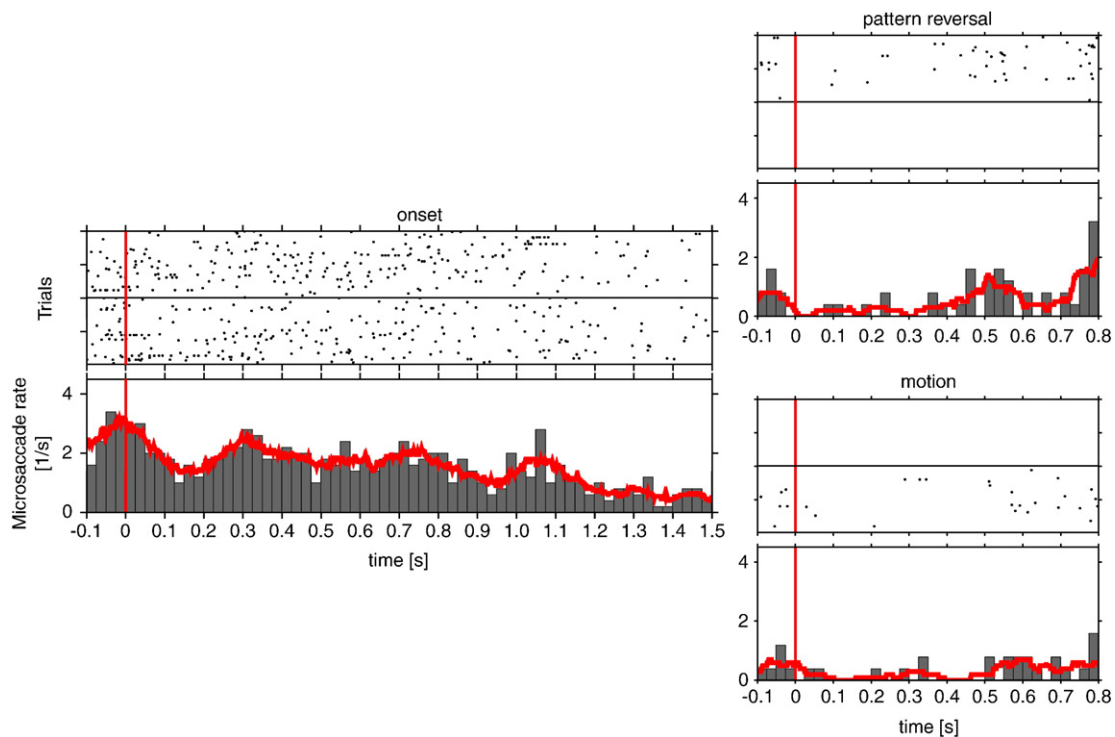


Fig. 4. Microsaccade rate of a representative subject (Experiment 2). The panels are arranged as follows: left panel shows the data of grating onset, and the right panels show the data of pattern reversal and motion, respectively. Top of the panels: raster plot of saccade onsets in all trials. Each row represents one trial (upper half: pattern reversal trials; lower half: motion trials). Black dots represent saccade onsets. The red vertical line represents the time point of grating onset, pattern reversal, and motion onset, respectively. Bottom of the panels: saccade rates per second in 25 ms bins. The red curve represents the saccades' rate (per second) smoothed with a moving time window of 100 ms. Note that the left panel in response to grating onset displays all trials, while the right panels represent only pattern reversal or motion, respectively, i.e., one half of the trials.

Following this decrease, the microsaccade rate increased to a maximum at about 480 ms after grating onset from which it slowly decreased below baseline level (see Fig. 3C, left panel). This time course is consistent with the common finding in research on microsaccades that the absolute frequency of microsaccades first drops shortly after the presentation of a visual stimulus (microsaccadic inhibition) and then displays a subsequent rebound (Engbert and Kliegl, 2003). Compared to grating onset, microsaccade rates at the onset of pattern reversal and motion were much lower with a decrease from about 0.5 saccades per second to near quiescence around 150–250 ms and a subsequent increase peaking about 800 ms following onset of display change (see Fig. 3C, middle and right panels). These time courses closely resemble the microsaccade rates caused by a motion direction change of a moving dot grid as reported by Laubrock et al. (2008).

A statistical evaluation of these qualitative descriptions by means of bootstrap analyses confirmed that the time course of microsaccades rate did not differ between the motion and the pattern reversal condition, whereas both conditions differed from the time course of the grating onset condition in the time window -100 to 540 ms (see Fig. 5). This difference in microsaccade rates is probably explained by differences in the display change between conditions. Since the initial onset of a static grating followed the presentation of a blank screen, the grating onset condition represented the appearance of a stimulus. On the other hand, both pattern reversal and motion onset occurred when a static grating was already present, therefore representing a change within an existing stimulus. Thus, our results show a higher microsaccade rate in response to the appearance of a stimulus (grating onset) compared with a change in stimulus properties (pattern reversal or motion) for both microsaccadic inhibition and subsequent rebound within 540 ms after onset of display change. Importantly, this pattern of results does not parallel the induced gamma-band results, which showed higher amplitudes for pattern reversal compared to motion, but no significant amplitude differences between grating onset and the other display conditions (see Fig. 3A and C). Furthermore, the peak latencies of the induced GBRs and the rebound of microsaccade rates did not coincide. It seems, therefore, unlikely that the differential modulations of the induced GBR are due to a concordant variation of microsaccade rate across conditions, as suggested by Yuval-Greenberg et al. (2008).

General discussion

The main issue of the current study was to investigate whether motion effects on the GBR reflect a special responsiveness of the GBR

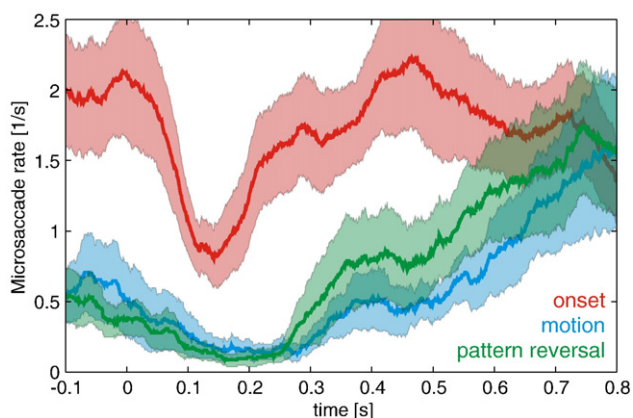


Fig. 5. Time course of microsaccades' rate (per second) with confidence intervals, Cl_{68} , obtained in a non-parametric bootstrap procedure as a function of display condition. The solid colored lines represent the mean values for each condition and the shaded regions represent ± 1 standard deviation, both computed by the bootstrap percentile method.

to the stimulus feature “motion,” or whether GBR enhancements of similar magnitude can be elicited also by a salient contrast change within a static grating that does not include motion. For this purpose, evoked and induced GBRs were analyzed in response to the onset of a static grating, a pattern reversal, and motion onset of the grating. In order to interpret the induced GBRs, we conducted a second experimental session, assessing the eye movement activity with an eye-tracking system during the same three display conditions employed for EEG measurements in the first experiment.

Evoked gamma-band response

In the present study, we found evoked GBRs for all three display conditions: (1) onset of a stationary grating, (2) pattern reversal of a static grating, and (3) motion onset of a previously static grating. This result is in general agreement with the role of the early evoked GBR in perceptual bottom-up processes (Başar-Eroglu et al., 1996; Herrmann et al., 2010). Evoked onset responses in the gamma-frequency range were also reported for stationary and moving gratings (Swettenham et al., 2009). For pattern reversal, the evoked GBR exhibited the highest amplitude and shortest latency, indicating stronger perceptual saliency and faster processing. In comparison to grating onset, the amplitude difference is probably explained by contrast effects, since inverting the black and white stripes in the pattern reversal condition reflects a stronger contrast change than a switch from a gray screen to the black and white stripes of the grating onset. Related to a population of neurons in the visual cortex, both grating onset and pattern reversal would activate 100% of the neurons' receptive fields responding to the contrast change of the grating, although to a different degree (stronger activation for pattern reversal). However, in the motion condition, only a fraction of the neurons are stimulated by contrast change at a given time point due to the spatiotemporal overlap of the single black and white stripes of the grating during the motion induction (see Fig. 6). Accordingly, also the weaker evoked GBR in the motion condition as compared to the pattern reversal condition can be related to a contrast-based explanation of evoked gamma-band activity changes (see Fig. 6), indicating that the GBR differences between the stimulus features “contrast change” and “motion” are more quantitative than qualitative in nature and reflect a bottom-up process inherent to all three stimulus conditions.

Such a contrast-related interpretation of the evoked GBR effects would be consistent with recent data from humans (Schadow et al., 2007) demonstrating gamma-band increases in response to increasing contrast levels of grating stimuli. It would also be consistent with the “match-and-utilization model” (MUM; Herrmann et al., 2004b), which suggests that visual input into early extrastriate cortex leads to an activation of higher visual areas, where perceptual memory representations are stored in the form of enhanced synaptic connections between and within visual areas. Input that matches such memory representations results in a rapid local feedback signal, which in turn leads to enhanced evoked gamma activity in the network. Although we do not assume differences between the stimulus conditions with regard to the memory match as such, the strength of the feedback signals should depend on input intensity (number of activated V1 neurons) and, therefore, lead to the observed evoked GBR differences, as demonstrated in a recent network simulation (Fründ et al., 2009).

We did not find a difference for evoked GBRs between grating onset and motion, which is consistent with findings of Swettenham et al. (2009). These authors also reported no differences of the evoked onset response between stationary and moving gratings. These results indicate that in terms of amplitude, the onset of a static grating represents a change of physical stimulus features that is comparable to the motion onset of this grating. With respect to latency, we found prolonged peak latencies for motion (122 ms) as compared to pattern reversal (74 ms) and grating onset (83 ms). The delayed GBR to

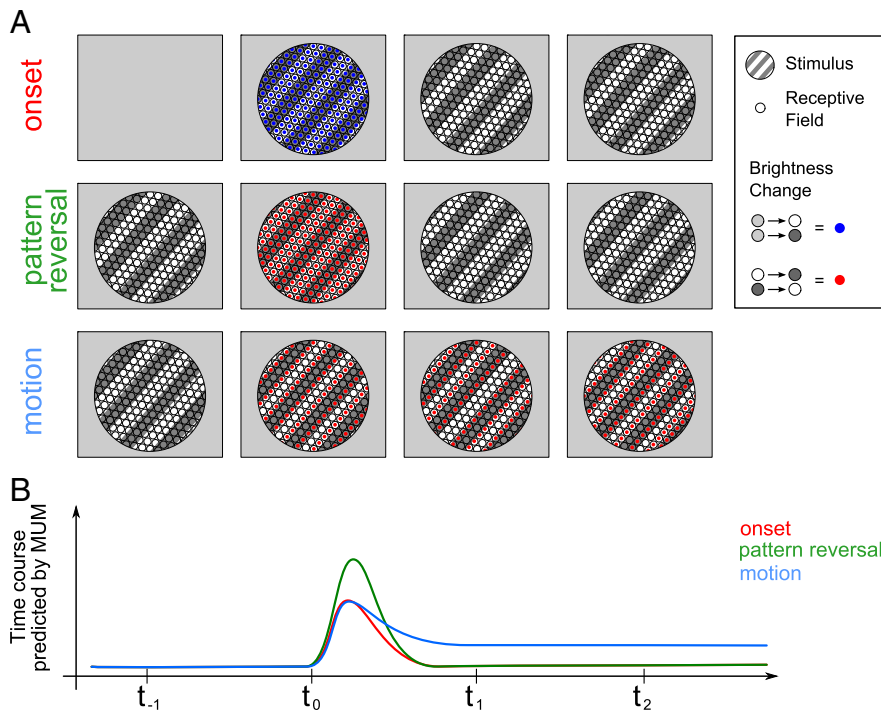


Fig. 6. (A) Schematic illustration of neuronal activation for different display conditions. Big grey rectangles with black-and-white-striped circles represent display and stimuli as utilized in the experiment. Open circles represent receptive fields of cortical neurons. Receptive fields stimulated by a brightness change from white to black or vice versa are marked with red dots; receptive fields stimulated by a brightness change from grey to white or grey to black are marked with blue dots. (B) Time course of activation as predicted by the MUM model as a function of display condition and time. At stimulus onset, all neurons respond to the change from a gray background to either white or black stripes. For a pattern reversal, the response is even stronger, since all neurons receive a stronger input when white stripes reverse to black and vice versa. For motion onset, the response is weaker than for pattern reversal, since only a fraction of the neurons are stimulated at each time. However, the motion response lasts longer, since each new frame of the movie again drives some neurons leading to a steady-state response.

motion might indicate a slower processing time due to higher discrimination difficulty (Senkowski and Herrmann, 2002). Moreover, the latency and amplitude differences between conditions are in line with findings from Fründ et al. (2007b), who reported lower evoked gamma-band amplitudes for responses with longer evoked gamma-band latencies. In addition, Fründ et al. (2007b) reported larger evoked gamma-band amplitudes and shorter latencies for fast compared to slow reaction times during a speeded reaction task. However, our behavioral data did not show significant differences in reaction times. This may be due to the fact that we did not instruct our subjects to react as fast as possible.

Induced gamma-band response and microsaccade rate

In addition to the early evoked GBR, we found a later GBR for all conditions, which was only present in the total GBR and therefore reflects the induced gamma-band activity. Induced GBRs have been suspected to be generated by microsaccades rather than reflecting neural responses (Yuval-Greenberg et al., 2008). Microsaccades are small, fast, jerk-like eye movements that are about 25 ms in duration and occur during voluntary fixation at an average rate of 1–2 per second (Martinez-Conde et al., 2004). Microsaccades are not randomly distributed over time. After stimulus onset, their rate drops temporarily below baseline but rebounds above baseline level between 200 and 400 ms (Engbert and Kliegl, 2003; Rolfs et al., 2008). Yuval-Greenberg et al. (2008) demonstrated that the typical transient amplitude increase of the EEG scalp-recorded induced GBR at about 200–300 ms after stimulus onset can be explained by this characteristic rebound of the microsaccade rate. Microsaccades are accompanied by extraocular muscle activity, which propagates to the EEG as a saccadic spike potential (Thickbroom and Mastaglia, 1986). When data are analyzed in the frequency domain, spike potentials translate to broadband artifacts in the EEG spectrum. Recent findings of

Dimigen et al. (2009) suggest that microsaccadic muscle spikes and the associated gamma-band artifacts are inevitably present in the raw EEG. According to the authors, this even holds under optimal conditions with precise fixation of a continuously shown fixation point and microsaccades with only half the size of those observed by Yuval-Greenberg et al. (2008).

Given these results, the induced GBRs reported here might reflect microsaccade related muscle activity, too. Since experimental conditions may differ in the relative number of microsaccades, which can mimic changes in induced gamma-band power, it is important to demonstrate that differences of GBR and microsaccade rate do not covary across conditions. We did exactly this by showing that the induced gamma-band modulations of Experiment 1 did not parallel the modulations of microsaccade rate obtained with the identical display conditions in Experiment 2. It is therefore rather unlikely that the induced GBRs we report here are artifacts of microsaccadic muscle potentials. This allows the following interpretations of our induced GBR.

To our knowledge, the only other human study using square-wave gratings to investigate motion-based gamma-band modulations was conducted by Swettenham et al. (2009). In this MEG study, stationary and moving gratings were presented for 2 s either in a fixed sequence within a trial (the stationary grating always preceded the drifting grating) or in separate randomized trials. For both conditions, the authors observed a sustained gamma-band oscillation throughout stimulus presentation that was centered at higher frequencies for moving as compared to stationary gratings. In the current study, we also found indications of a sustained GBR for static and moving gratings (see Fig. 3A). This is in line with the MUM model (Herrmann et al., 2004b), which predicts induced GBRs when previously extracted information is utilized for further processing. In the present study, the onset of the grating can be considered as a cue for behaviorally responding to the subsequently presented stimuli

(pattern reversal or motion onset). Thus, during this phase of the experiment, a high level of attention has to be maintained by the participants, resulting in the sustained induced GBR.

Also with respect to frequency, our results are in agreement with the findings of Swettenham et al. (2009). We observed a gamma-frequency increase of ~10 Hz in response to moving compared to stationary gratings, indicating that the encoding of moving gratings in early visual cortex is reflected by an upward frequency shift. However, irrespective of the relative frequency difference between conditions, absolute frequencies per condition were higher in our study (stationary: 53.2 Hz; moving: 62.8 Hz) than in the study of Swettenham et al. (stationary: 44 Hz; moving: 51 Hz). This discrepancy might be related to differences in the velocity of the grating movement. We presented the gratings with a slightly higher velocity (1.75°/s) than Swettenham et al. (1.33°/s), and it has been shown in animal studies that gamma-frequency increases with stimulus velocity (Gray et al., 1990; Gray and Viana Di Prisco, 1997). Similarly, Friedman-Hill et al. (2000) reported higher gamma-frequency responses for moving gratings compared to static ones in the awake monkey. These authors hypothesize that their observation of low-frequency oscillations in response to stationary stimuli may simply represent the lower end-point of the speed spectrum. Our results are also consistent with a human MEG study (Siegel et al., 2007), demonstrating an important role for sustained high gamma-frequencies in motion discrimination. These authors analyzed different frequency bands in response to random dot kinematograms of different motion coherence and found the most reliable increase of responses with visual motion strength for the high gamma-band from about 60 to 100 Hz.

With respect to amplitude differences, our results showed higher induced GBRs for pattern reversal compared to motion. As it was the case for the early evoked GBR, this finding indicates that also the late induced GBR is more strongly modulated by a contrast change than by motion. This is in line with a modulation of late induced GBRs by bottom-up contrast processing, as has been demonstrated in human MEG (Hall et al., 2005) and EEG studies (Fründ et al., 2008; Koch et al., 2009).

However, we did not observe an amplitude difference between the stationary grating in the grating onset condition and the drifting grating in the motion condition. This is, at least partly, in contrast to the findings of Swettenham et al. (2009), who observed an amplitude increase for moving compared with static gratings only when they presented the stationary and moving gratings always in the same order, but not when stimuli were presented in separate randomized trials. In the current study, we used a pseudorandomized trial order to avoid confounding effects of anticipation and task expectancy because it has been demonstrated that the state of anticipation enhances the gamma-band power (Fitzgibbon et al., 2004; Schadow et al., 2009). Furthermore, in contrast to our study, Swettenham et al. (2009) did not use an eye tracker, leaving the possibility that differences in GBRs between moving and stationary gratings might reflect differences in microsaccade rates between conditions (Yuval-Greenberg et al., 2008).

Conclusions

The present study demonstrated that a sudden contrast change within a static grating elicits stronger evoked and induced GBRs than moving gratings, indicating that grating-based GBR modulations in early visual cortex are not motion-specific. However, mean frequencies of the induced GBR were higher in response to moving compared to stationary gratings, indicating that the encoding of moving gratings in early vision is reflected by frequency modulation within the high gamma-band. Since the reported modulations of the induced GBR did not parallel the modulations of microsaccade rate, we argue that our induced GBRs reflect neuronal processes.

Acknowledgments

We wish to thank all participants in this study for their time, patience, and effort. The work described was supported by the Honda Research Institute Europe.

References

- Adrian, E.D., 1942. Olfactory reactions in the brain of the hedgehog. *J. Physiol.* 100, 459–473.
- Axmacher, N., Mormann, F., Fernández, G., Cohen, M.X., Elger, C.E., Fell, J., 2007. Sustained neural activity patterns during working memory in the human medial temporal lobe. *J. Neurosci.* 27, 7807–7816.
- Axmacher, N., Mormann, F., Fernández, G., Elger, C.E., Fell, J., 2006. Memory formation by neuronal synchronization. *Brain Res. Rev.* 52, 170–182.
- Başar, E., Gönder, A., Ugan, P., 1980. Comparative frequency analysis of single EEG-evoked potential records. *J. Biomed. Eng.* 2, 9–14.
- Başar-Eroglu, C., Strüber, D., Schürmann, M., Stadler, M., Başar, E., 1996. Gamma-band responses in the brain: a short review of psychophysiological correlates and functional significance. *Int. J. Psychophysiol.* 24, 101–112.
- Busch, N.A., Debener, S., Kranczioch, C., Engel, A.K., Herrmann, C.S., 2004. Size matters: effects of stimulus size, duration and eccentricity on the visual gamma-band response. *Clin. Neurophysiol.* 115, 1810–1820.
- Busch, N.A., Groh-Bordin, C., Zimmer, H.D., Herrmann, C.S., 2008. Modes of memory: early electrophysiological markers of repetition suppression and recognition enhancement predict behavioral performance. *Psychophysiology* 45, 25–35.
- Busch, N.A., Schadow, J., Fründ, I., Herrmann, C.S., 2006. Time-frequency analysis of target detection reveals an early interface between bottom-up and top-down processes in the gamma-band. *Neuroimage* 29, 1106–1116.
- Debener, S., Herrmann, C.S., Kranczioch, C., Gembris, D., Engel, A.K., 2003. Top-down attentional processing enhances auditory evoked gamma band activity. *NeuroReport* 14, 683–686.
- Demiralp, T., Başar-Eroglu, C., Başar, E., 1996. Distributed gamma band responses in the brain studied in cortex, reticular formation, hippocampus and cerebellum. *Int. J. Neurosci.* 84, 1–13.
- Dimigen, O., Valsecchi, M., Sommer, W., Kliegl, R., 2009. Human microsaccade-related visual brain responses. *J. Neurosci.* 29, 12321–12331.
- Eckhorn, R., 1999. Neural mechanisms of visual feature binding investigated with microelectrodes and models. *Vis. Cogn.* 6, 231–265.
- Efron, B., Tibshirani, R., 1986. Bootstrap methods for standard errors, confidence intervals, and other measures of statistical accuracy. *Stat. Sci.* 1, 54–75.
- Engbert, R., Kliegl, R., 2003. Microsaccades uncover the orientation of covert attention. *Vis. Res.* 43, 1035–1045.
- Engbert, R., Mergenthaler, K., 2006. Microsaccades are triggered by low retinal image slip. *Proc. Natl Acad. Sci. USA* 103, 7192–7197.
- Engel, A.K., Fries, P., Singer, W., 2001. Dynamic predictions: oscillations and synchrony in top-down processing. *Nat. Rev. Neurosci.* 2, 704–716.
- Engel, A.K., Roelfsema, P.R., Fries, P., Brecht, M., Singer, W., 1997. Role of the temporal domain for response selection and perceptual binding. *Cereb. Cortex* 7, 571–582.
- Fell, J., Fernández, G., Klaver, P., Elger, C.E., Fries, P., 2003. Is synchronized neuronal gamma activity relevant for selective attention? *Brain Res. Brain Res. Rev.* 42, 265–272.
- Fitzgibbon, S.P., Pope, K.J., Mackenzie, L., Clark, C.R., Willoughby, J.O., 2004. Cognitive tasks augment gamma EEG power. *Clin. Neurophysiol.* 115, 1802–1809.
- Friedman-Hill, S., Maldonado, P.E., Gray, C.M., 2000. Dynamics of striate cortical activity in the alert macaque: I. Incidence and stimulus-dependence of gamma-band neuronal oscillations. *Cereb. Cortex* 10, 1105–1116.
- Fries, P., Reynolds, J.H., Rorie, A.E., Desimone, R., 2001. Modulation of oscillatory neuronal synchronization by selective visual attention. *Science* 291, 1560–1563.
- Fründ, I., Busch, N.A., Körner, U., Schadow, J., Herrmann, C.S., 2007a. EEG oscillations in the gamma and alpha range respond differently to spatial frequency. *Vis. Res.* 47, 2086–2098.
- Fründ, I., Busch, N.A., Schadow, J., Körner, U., Herrmann, C.S., 2007b. From perception to action: phase-locked gamma oscillations correlate with reaction times in a speeded response task. *BMC Neurosci.* 8, 27.
- Fründ, I., Ohl, F.W., Herrmann, C.S., 2009. Spike-timing-dependent plasticity leads to gamma band responses in a neural network. *Biol. Cybern.* 101, 227–240.
- Fründ, I., Schadow, J., Busch, N.A., Naue, N., Körner, U., Herrmann, C.S., 2008. Anticipation of natural stimuli modulates EEG dynamics: physiology and simulation. *Cogn. Neurodyn.* 2, 89–100.
- Gray, C.M., 1999. The temporal correlation hypothesis of visual feature integration: still alive and well. *Neuron* 24 (31–47), 111–125.
- Gray, C.M., Engel, A.K., König, P., Singer, W., 1990. Stimulus-dependent neuronal oscillations in cat visual cortex: receptive field properties and feature dependence. *Eur. J. Neurosci.* 2, 607–619.
- Gray, C.M., Viana Di Prisco, G., 1997. Stimulus-dependent neuronal oscillations and local synchronization in striate cortex of the alert cat. *J. Neurosci.* 17, 3239–3253.
- Gruber, T., Keil, A., Müller, M.M., 2001. Modulation of induced gamma band responses and phase synchrony in a paired associate learning task in the human EEG. *Neurosci. Lett.* 316, 29–32.
- Gruber, T., Müller, M.M., 2005. Oscillatory brain activity dissociates between associative stimulus content in a repetition priming task in the human EEG. *Cereb. Cortex* 15, 109–116.

- Gruber, T., Müller, M.M., 2006. Oscillatory brain activity in the human EEG during indirect and direct memory tasks. *Brain Res.* 1097, 194–204.
- Gruber, T., Müller, M.M., Keil, A., Elbert, T., 1999. Selective visual-spatial attention alters induced gamma band responses in the human EEG. *Clin. Neurophysiol.* 110, 2074–2085.
- Gruber, T., Tsivilis, D., Montaldi, D., Müller, M.M., 2004. Induced gamma band responses: an early marker of memory encoding and retrieval. *NeuroReport* 15, 1837–1841.
- Hall, S.D., Holliday, I.E., Hillebrand, A., Singh, K.D., Furlong, P.L., Hadjipapas, A., Barnes, G.R., 2005. The missing link: analogous human and primate cortical gamma oscillations. *Neuroimage* 26, 13–17.
- Herrmann, C.S., Fründ, I., Lenz, D., 2010. Human gamma-band activity: a review on cognitive and behavioral correlates and network models. *Neurosci. Biobehav. Rev.* 34, 981–992.
- Herrmann, C.S., Lenz, D., Junge, S., Busch, N.A., Maess, B., 2004a. Memory-matches evoke human gamma-responses. *BMC Neurosci.* 5, 13.
- Herrmann, C.S., Mecklinger, A., Pfeifer, E., 1999. Gamma responses and ERPs in a visual classification task. *Clin. Neurophysiol.* 110, 636–642.
- Herrmann, C.S., Munk, M.H.J., Engel, A.K., 2004b. Cognitive functions of gamma-band activity: memory match and utilization. *Trends Cogn. Sci.* 8, 347–355.
- Koch, S.P., Werner, P., Steinbrink, J., Fries, P., Obrig, H., 2009. Stimulus-induced and state-dependent sustained gamma activity is tightly coupled to the hemodynamic response in humans. *J. Neurosci.* 29, 13962–13970.
- Krishnan, G.P., Skosnik, P.D., Vohs, J.L., Busey, T.A., O'Donnell, B.F., 2005. Relationship between steady-state and induced gamma activity to motion. *NeuroReport* 16, 625–630.
- Kruse, W., Eckhorn, R., 1996. Inhibition of sustained gamma oscillations (35–80 Hz) by fast transient responses in cat visual cortex. *Proc. Natl Acad. Sci. USA* 93, 6112–6117.
- Lachaux, J.-P., George, N., Tallon-Baudry, C., Martinerie, J., Hugueville, L., Minotti, L., Kahane, P., Renault, B., 2005. The many faces of the gamma band response to complex visual stimuli. *Neuroimage* 25, 491–501.
- Laubrock, J., Engbert, R., Kliegl, R., 2008. Fixational eye movements predict the perceived direction of ambiguous apparent motion. *J. Vis.* 8, 13.1–13.17.
- Lutzenberger, W., Pulvermüller, F., Elbert, T., Birbaumer, N., 1995. Visual stimulation alters local 40-Hz responses in humans: an EEG-study. *Neurosci. Lett.* 183, 39–42.
- Martinez-Conde, S., Macknik, S.L., Hubel, D.H., 2004. The role of fixational eye movements in visual perception. *Nat. Rev. Neurosci.* 5, 229–240.
- Martinovic, J., Gruber, T., Hantsch, A., Müller, M.M., 2008. Induced gamma-band activity is related to the time point of object identification. *Brain Res.* 1198, 93–106.
- Miltner, W.H., Braun, C., Arnold, M., Witte, H., Taub, E., 1999. Coherence of gamma-band EEG activity as a basis for associative learning. *Nature* 397, 434–436.
- Müller, M.M., Junghöfer, M., Elbert, T., Rochstroh, B., 1997. Visually induced gamma-band responses to coherent and incoherent motion: a replication study. *NeuroReport* 8, 2575–2579.
- Ohla, K., Busch, N.A., Herrmann, C.S., 2007. Early electrophysiological markers of visual awareness in the human brain. *Neuroimage* 37, 1329–1337.
- Rolfs, M., Kliegl, R., Engbert, R., 2008. Toward a model of microsaccade generation: the case of microsaccadic inhibition. *J. Vis.* 8, 5.1–5.23.
- Schadow, J., Lenz, D., Dettler, N., Fründ, I., Herrmann, C.S., 2009. Early gamma-band responses reflect anticipatory top-down modulation in the auditory cortex. *Neuroimage* 47, 651–658.
- Schadow, J., Lenz, D., Thaeig, S., Busch, N.A., Fründ, I., Rieger, J.W., Herrmann, C.S., 2007. Stimulus intensity affects early sensory processing: visual contrast modulates evoked gamma-band activity in human EEG. *Int. J. Psychophysiol.* 66, 28–36.
- Schanze, T., Eckhorn, R., 1997. Phase correlation among rhythms present at different frequencies: spectral methods, application to microelectrode recordings from visual cortex and functional implications. *Int. J. Psychophysiol.* 26, 171–189.
- Sederberg, P.B., Kahana, M.J., Howard, M.W., Donner, E.J., Madsen, J.R., 2003. Theta and gamma oscillations during encoding predict subsequent recall. *J. Neurosci.* 23, 10809–10814.
- Senkowski, D., Herrmann, C.S., 2002. Effects of task difficulty on evoked gamma activity and ERPs in a visual discrimination task. *Clin. Neurophysiol.* 113, 1742–1753.
- Siegel, M., Donner, T.H., Oostenveld, R., Fries, P., Engel, A.K., 2007. High-frequency activity in human visual cortex is modulated by visual motion strength. *Cereb. Cortex* 17, 732–741.
- Singer, W., Gray, C.M., 1995. Visual feature integration and the temporal correlation hypothesis. *Annu. Rev. Neurosci.* 18, 555–586.
- Swettenham, J.B., Muthukumaraswamy, S.D., Singh, K.D., 2009. Spectral properties of induced and evoked gamma oscillations in human early visual cortex to moving and stationary stimuli. *J. Neurophysiol.* 102, 1241–1253.
- Tallon-Baudry, Bertrand, 1999. Oscillatory gamma activity in humans and its role in object representation. *Trends Cogn. Sci.* 3, 151–162.
- Tallon-Baudry, C., Bertrand, O., Hénaff, M.-A., Isnard, J., Fischer, C., 2005. Attention modulates gamma-band oscillations differently in the human lateral occipital cortex and fusiform gyrus. *Cereb. Cortex* 15, 654–662.
- Thickbroom, G.W., Mastaglia, F.L., 1986. Presaccadic spike potential. relation to eye movement direction. *Electroencephalogr. Clin. Neurophysiol.* 64, 211–214.
- Yuval-Greenberg, S., Tomer, O., Keren, A.S., Nelken, I., Deouell, L.Y., 2008. Transient induced gamma-band response in EEG as a manifestation of miniature saccades. *Neuron* 58, 429–441.
- Zaehle, T., Fründ, I., Schadow, J., Thärig, S., Schoenfeld, M.A., Herrmann, C.S., 2009. Inter- and intra-individual covariations of hemodynamic and oscillatory gamma responses in the human cortex. *Front. Hum. Neurosci.* 3, 8.